Cell

A Cell-Surface Receptor for Lipocalin 24p3 Selectively Mediates Apoptosis and Iron Uptake

Laxminarayana R. Devireddy,[1,2] Claude Gazin,[1,2] Xiaochun Zhu,[1] and Michael R. Green[1,*]
[1] Howard Hughes Medical Institute, Programs in Gene Function and Expression and Molecular Medicine, University of Massachusetts Medical School, Worcester, MA 01605, USA
[2] These authors contributed equally to this work.
*Contact: michael.green@umassmed.edu
DOI 10.1016/j.cell.2005.10.027

SUMMARY

The lipocalin mouse 24p3 has been implicated in diverse physiological processes, including apoptosis due to interleukin-3 (IL-3) deprivation and iron transport. Here we report cloning of the 24p3 cell-surface receptor (24p3R). Ectopic 24p3R expression confers on cells the ability to undergo either iron uptake or apoptosis, dependent upon the iron content of the ligand: Iron-loaded 24p3 increases intracellular iron concentration without promoting apoptosis; iron-lacking 24p3 decreases intracellular iron levels, which induces expression of the proapoptotic protein Bim, resulting in apoptosis. Intracellular iron delivery blocks Bim induction and suppresses apoptosis due to 24p3 addition or IL-3 deprivation. We find, unexpectedly, that the BCR-ABL oncoprotein activates expression of *24p3* and represses *24p3R* expression, rendering BCR-ABL$^+$ cells refractory to secreted 24p3. By inhibiting BCR-ABL, imatinib induces *24p3R* expression and, consequently, apoptosis. Our results reveal an unanticipated role for intracellular iron regulation in an apoptotic pathway relevant to BCR-ABL-induced myeloproliferative disease and its treatment.

INTRODUCTION

Apoptosis is a physiological form of cell death that has been broadly implicated in disparate biological processes, including normal development, tissue homeostasis, and defense against pathogens (reviewed in Datta et al., 1999; Vaux and Korsmeyer, 1999). There is substantial evidence that certain apoptotic programs are transcriptionally regulated. For example, the p53 tumor suppressor pathway induces apoptosis, at least in part, by transcriptional activation of p53-dependent genes (Polyak et al., 1997). Other transcription-dependent apoptotic programs include glucocorticoid-induced killing of thymocytes (Cohen and Duke, 1984; Galili et al., 1982) and cell death induced by signaling through the T cell receptor (Lenardo et al., 1999).

In some cells, apoptosis is induced by deprivation of trophic factors. For example, many hematopoietic cells undergo apoptosis when deprived of a specific cytokine such as interleukin 3 (IL-3). Significantly, apoptosis induced by IL-3 withdrawal can be blocked by the transcription inhibitor actinomycin D or the translation inhibitor cycloheximide, implying a requirement for gene expression (Ishida et al., 1992).

Using DNA microarrays to analyze IL-3-dependent murine pro-B lymphocytic FL5.12 cells, we found that the gene undergoing maximal transcriptional induction following cytokine withdrawal is the lipocalin *24p3* (also called lipocalin 2) (Devireddy et al., 2001). Lipocalins are a family of secreted proteins that can bind small molecular weight ligands (Akerstrom et al., 2000; Flower, 1996) and have diverse molecular recognition properties and functions including retinol transport, cryptic coloration, olfaction, pheromone transport, and prostaglandin synthesis (reviewed in Akerstrom et al., 2000; Flower, 1996).

We have previously shown that conditioned medium (CM) from IL-3-deprived FL5.12 cells contains 24p3 and induces apoptosis of naïve FL5.12 cells even when IL-3 is present (Devireddy et al., 2001). Furthermore, CM from IL-3-deprived FL5.12 cells or COS-7 cells expressing 24p3, as well as purified 24p3, induces apoptosis in a variety of hematopoietic cells. Based upon these results, we have proposed that IL-3 deprivation activates *24p3* transcription, leading to synthesis and secretion of 24p3, which induces apoptosis through an autocrine/paracrine pathway.

Recently, several studies have found that 24p3 can bind iron and deliver it to cells (Goetz et al., 2002; Yang et al., 2002, 2003). 24p3 does not have an intrinsic ability to interact with iron, but iron is instead bound through a 24p3-associated small molecular weight siderophore (Goetz et al.,

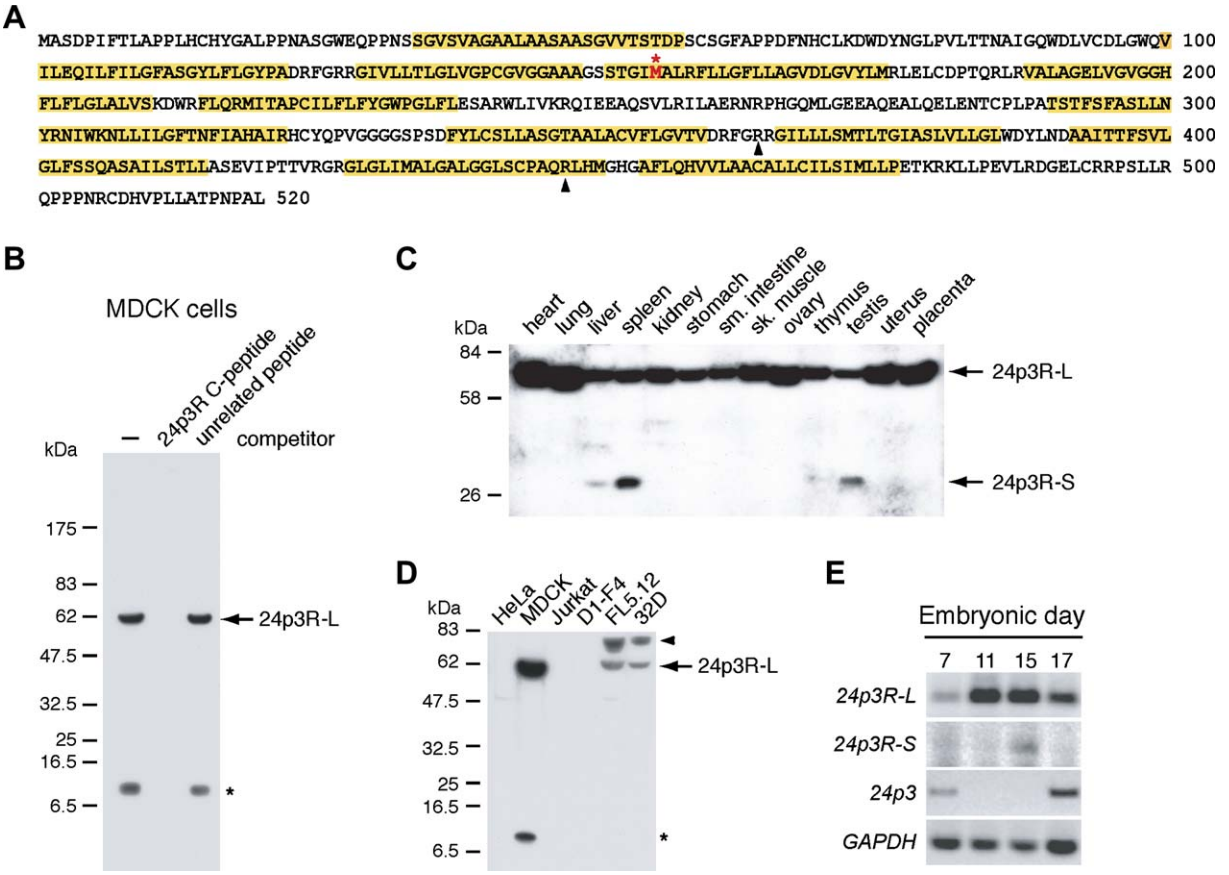

Figure 1. Sequence and Expression Analysis of 24p3R

(A) Full-length sequence of the murine 24p3R. Highlighted sequences represent putative transmembrane domains. The asterisk denotes the initiating methionine of the short form of 24p3R, 24p3R-S. Arrowheads indicate the N-terminal boundary of the isolated 24p3-interacting clones.

(B) Characterization of the α-24p3R antibody. Immunoblot analysis in MDCK cells using an α-24p3R antibody incubated with excess immunogenic peptide or an unrelated peptide. The asterisk indicates proteolytic products of 24p3R.

(C and D) Immunoblot analysis on a panel of murine tissues (C) and cell lines (D). A higher molecular weight form of 24p3R is indicated by the arrowhead.

(E) RT-PCR analysis monitoring expression of *24p3R-L*, *24p3R-S*, *24p3,* and, as a control, *GAPDH* in whole embryos during different stages of mouse development.

2002; Yang et al., 2002). Following cellular uptake of 24p3 by endocytosis, the bound iron is released, resulting in an increased intracellular iron concentration (Yang et al., 2002).

The observation that 24p3 is a secreted protein that is internalized through an endocytotic mechanism suggests the existence of a 24p3 cell-surface receptor. Here we report the isolation of a 24p3 cell-surface receptor and show how a single receptor can mediate diverse physiological processes dependent upon the state of the ligand and independent of cell type.

RESULTS

Isolation of a 24p3 Cell-Surface Receptor

To isolate a cell-surface receptor for 24p3 (24p3R), we performed expression cloning using a cDNA library prepared from murine FL5.12 cells, which are highly sensitive to 24p3-mediated apoptosis (Devireddy et al., 2001). The cDNA library was transfected into COS-7 cells and, after three rounds of panning, two clones were identified that conferred maximal 24p3 binding activity. DNA sequence analysis revealed that the two clones contained an overlapping DNA sequence, which matched a database entry proposed to encode a murine protein named brain type organic cation transporter (BOCT) (GenBank accession number NM_021551). Database searches also revealed the presence of a highly conserved human homolog (NM_016609). The full-length murine cDNA contained a single open reading frame of 520 amino acids that is predicted to contain 12 transmembrane helices (Figure 1A).

To determine the expression pattern of 24p3R, we raised and affinity-purified a polyclonal antibody using as an immunogen a C-terminal 24p3R peptide. The α-24p3R antibody detected a 60 kDa polypeptide in MDCK kidney epithelial cells (Figure 1B) as well as other cell lines and murine tissues (see below), consistent with the predicted size of 24p3R. Figure 1B shows that detection of the 60 kDa polypeptide

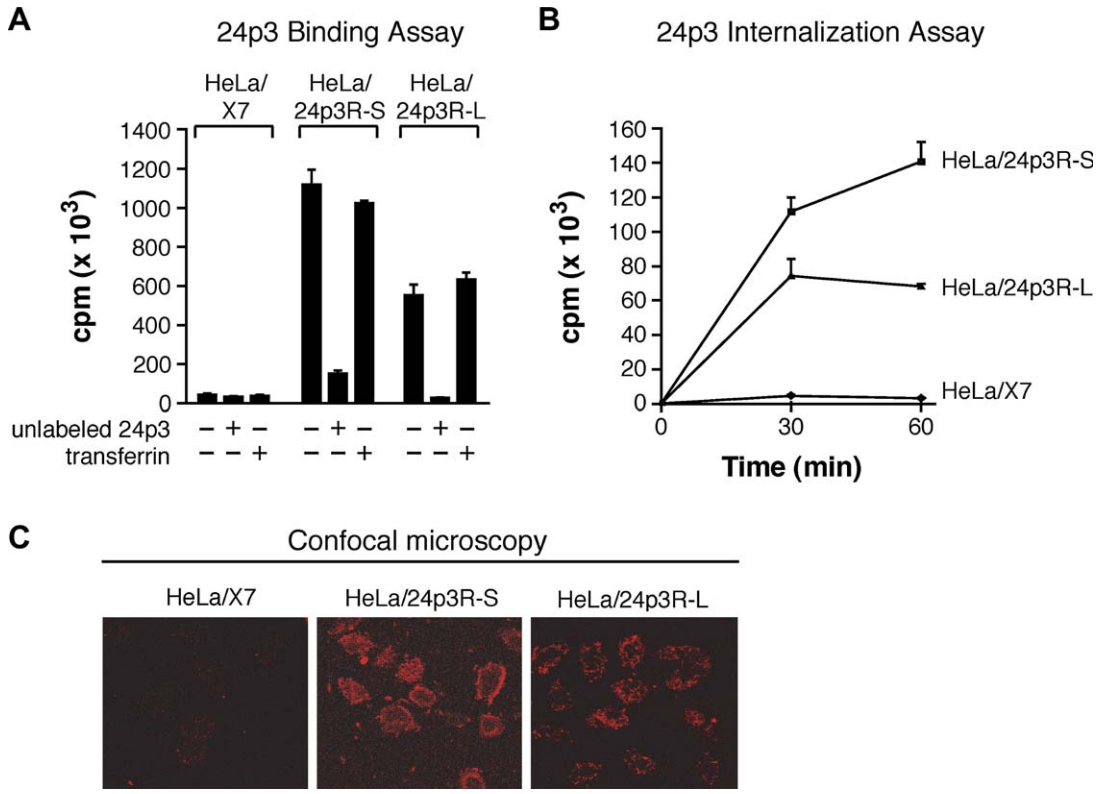

Figure 2. HeLa Cells Stably Expressing 24p3R Bind and Internalize 24p3

(A) Ligand-cell binding experiments. HeLa cells stably expressing 24p3R-S (HeLa/24p3R-S), 24p3R-L (HeLa/24p3R-L), or the empty expression vector (HeLa/X7) were incubated with ^{32}P-labeled 24p3 as previously described (Devireddy et al., 2001) together with excess unlabeled 24p3 or transferrin. Error bars represent standard deviation.

(B) 24p3 internalization assay. Cells were incubated with ^{32}P-labeled 24p3 and at various time-points protease treated, collected, washed, and counted.

(C) 24p3 localization. Cells were incubated with 24p3-Alexa568, fixed, and analyzed by confocal microscopy.

was blocked by incubation of the antiserum with the peptide immunogen but not an unrelated peptide.

Immunoblot analysis on a panel of murine tissues revealed that 24p3R was widely expressed (Figure 1C). Several tissues, such as spleen and testis, had a smaller, ~30 kDa form of 24p3R. RT-PCR analysis and EST database searches (data not shown) indicated that this shorter form represented an alternatively spliced variant lacking the N-terminal 154 amino acids (Figure 1A). We will refer to these forms as 24p3R-long (24p3R-L) and 24p3R-short (24p3R-S). Immunoblot analysis of a panel of cell lines revealed that 24p3R-L was expressed in MDCK, FL5.12, and 32D (IL-3-dependent murine myeloid) cells but not in HeLa cells (Figure 1D). FL5.12 and 32D cells also expressed a higher molecular weight form of 24p3R. Significantly, 24p3R was not expressed in human Jurkat or murine D1-F4 cells, two hematopoietic cell lines that are atypically resistant to 24p3-mediated apoptosis (Devireddy et al., 2001). RT-PCR analysis during different mouse embryonic stages revealed that *24p3R-L* was expressed as early as day 7 and persisted throughout development (Figure 1E).

We next asked whether ectopically expressed 24p3R was able to bind and mediate internalization of 24p3. As described above, 24p3R is not detectably expressed in HeLa cells. To perform functional experiments, we derived HeLa cell lines stably expressing 24p3R-S and 24p3R-L (HeLa/24p3R-S and HeLa/24p3R-L) and, as a control, the empty expression vector (HeLa/X7). The ligand-cell binding experiments of Figure 2A show that ^{32}P-labeled 24p3 bound to HeLa/24p3R-S and HeLa/24p3R-L cells but not to HeLa/X7 cells. Binding of ^{32}P-labeled 24p3 to HeLa/24p3R-S and HeLa/24p3R-L cells was blocked by addition of excess unlabeled 24p3 but not the unrelated protein, transferrin. Scatchard analysis indicates that 24p3R-S has a slightly higher affinity than 24p3R-L for 24p3 (data not shown).

Following addition to cells, 24p3 (Yang et al., 2002) and other lipocalins (Wojnar et al., 2003; Yang et al., 2002) are internalized by endocytosis. Figure 2B shows that ^{32}P-labeled 24p3 was internalized following addition to HeLa/24p3R-S and HeLa/24p3R-L but not to HeLa/X7 cells. Likewise, Figure 2C shows that Alexa568-derivatized 24p3 (24p3-Alexa568) accumulated at the surface and within HeLa/24p3R-S and HeLa/24p3R-L but not within HeLa/X7 cells. Collectively, the results of Figure 2 show that ectopic expression of 24p3R confers on HeLa cells the ability to bind and internalize 24p3.

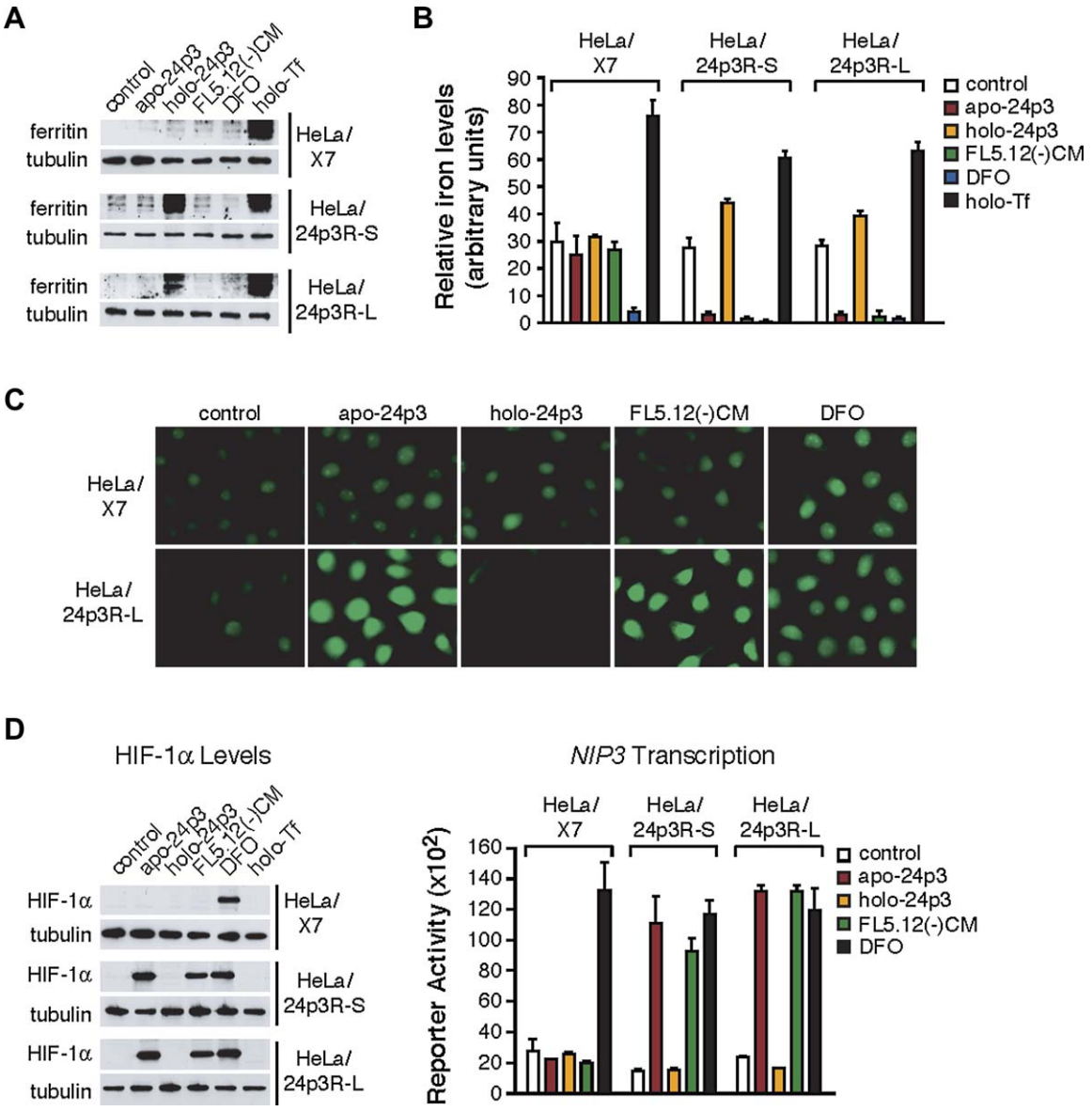

Figure 3. Depletion of Intracellular Iron by Apo-24p3 in Cells Expressing 24p3R

(A) Analysis of intracellular iron concentration by monitoring expression of ferritin protein levels by immunoblotting in untreated cells (control) or cells treated with recombinant iron-lacking 24p3 (apo-24p3), recombinant iron-loaded 24p3 (holo-24p3), CM from IL-3-deprived FL5.12 cells [FL5.12(-)CM], desferrioxamine (DFO), or holo-transferrin (holo-Tf). Tubulin levels were also monitored as a control.

(B) Colorimetric analysis of intracellular iron concentration. Error bars represent standard deviation.

(C) Determination of intracellular iron concentration by fluorescence calcein assay.

(D) Determination of intracellular iron concentration by immunoblot analysis of HIF-1α expression (left) and *NIP3* transcription by luciferase reporter gene activity (right).

24p3-Mediated Iron Uptake in Cells Expressing 24p3R

We next asked whether ectopic 24p3R expression would confer on HeLa cells the ability to uptake iron in a ligand-dependent fashion. In these experiments as well as those described below, we compared three preparations of 24p3: recombinant iron-loaded 24p3 (holo-24p3), recombinant iron-lacking 24p3 (apo-24p3), and CM from IL-3-deprived FL5.12 cells, which contains 24p3 [FL5.12(-)CM] (Devireddy et al., 2001). The three preparations of 24p3 were added to HeLa/24p3R-S, HeLa/24p3R-L, or HeLa/X7 cells, in parallel with iron-containing transferrin (holo-Tf) and the membrane-permeable iron chelator desferrioxamine (DFO) as controls.

To monitor intracellular iron concentration, we analyzed by immunoblotting the level of ferritin protein; translation of ferritin mRNA is iron regulated (Rouault and Klausner, 1997).

The results of Figure 3A show, as expected, that holo-Tf increased intracellular iron concentration in all three HeLa cell lines, as evidenced by enhanced levels of ferritin protein. Significantly, holo-24p3 also increased intracellular iron concentration in HeLa/24p3R-S and HeLa/24p3R-L but not in HeLa/X7 cells. By contrast, addition of apo-24p3, FL5.12(-)CM, or DFO did not increase intracellular iron in any of the three cell lines.

To confirm these results, we used a colorimetric assay to measure intracellular iron concentration (Leardi et al., 1998). Figure 3B shows that addition of holo-24p3 increased intracellular iron in HeLa/24p3R-S and HeLa/24p3R-L cells but not in HeLa/X7 cells. Unexpectedly, addition of apo-24p3 and FL5.12(-)CM substantially reduced intracellular iron concentration in HeLa/24p3R-S and HeLa/24p3R-L cells. Collectively, the results of Figures 3A and 3B indicate that 24p3R can mediate intracellular iron delivery by holo-24p3.

Depletion of Intracellular Iron by Apo-24p3 in Cells Expressing 24p3R

The results of Figure 3B raised the possibility that apo-24p3 acted as an iron chelator to lower intracellular iron concentration. To confirm this idea, we performed a second assay that measured intracellular iron levels using the iron sensor dye, calcein. Calcein is a fluorescent, cell-permeable dye whose emission is quenched by iron binding (Epsztejn et al., 1997). The results of Figure 3C show that in calcein-loaded HeLa/24p3R-L cells, there was an increase in fluorescence emission following addition of apo-24p3 and FL5.12(-)CM, indicating a decrease in intracellular free iron. We also analyzed the expression of two genes, *HIF-1α* and *NIP3*, which are upregulated following a decrease in intracellular iron concentration (Chong et al., 2002). The results of Figure 3D show that apo-24p3 and FL5.12(-)CM increased HIF-1α protein levels (left) and *NIP3* transcription (right) in HeLa/24p3R-S and HeLa/24p3R-L but not in HeLa/X7 cells. As expected, DFO induced expression of HIF-1α and *NIP3* in all three cell lines.

We next investigated the pathway by which apo-24p3 lowers intracellular iron levels. HeLa/X7 and HeLa/24p3R-L cells were preincubated with ^{55}Fe, recultured in fresh medium lacking ^{55}Fe, and then treated with apo-24p3. We first confirmed that 24p3 bound intracellular ^{55}Fe by immunoprecipitation of cell lysates. The results of Figure 4A show that there was substantial association of ^{55}Fe with 24p3 in HeLa/24p3R-L but not in HeLa/X7 cells. We next asked whether 24p3 simply sequestered intracellular iron or transferred it to the extracellular medium. HeLa/X7 and HeLa/24p3R-L cells were preincubated with ^{55}Fe, recultured in fresh medium lacking ^{55}Fe, treated with apo-24p3 or, as a control, DFO, and the accumulation of ^{55}Fe in the medium was determined by liquid scintillation counting. Figure 4B shows that addition of apo-24p3 or DFO to HeLa/24p3R-L cells led to a time-dependent accumulation of ^{55}Fe in the medium. By contrast, in HeLa/X7 cells only DFO affected the distribution of ^{55}Fe. To verify that ^{55}Fe was transferred outside the cell by 24p3, HeLa/X7 and HeLa/24p3R-L cells were treated as described above and, after 24 hr, the cells were washed to remove any residual extracellular apo-24p3 and newly secreted ^{55}Fe-associated 24p3 was analyzed by immunoprecipitation. Figure 4C shows that ^{55}Fe-associated 24p3 accumulated in the extracellular medium. Collectively, these results indicate that in cells expressing 24p3R, apo-24p3 is internalized, binds to intracellular ^{55}Fe, and transfers it to the extracellular medium, resulting in decreased intracellular iron levels.

We considered the possibility that 24p3 exited the cell through an endosome recycling pathway, as occurs for several other endocytosed receptor-ligand complexes (Maxfield and McGraw, 2004). As a first test of this idea, we asked whether intracellular 24p3 was present in recycling endosomes as evidenced by colocalization with Rab11, a well-established recycling endosome marker (Maxfield and McGraw, 2004). HeLa/24p3R-L cells were transfected with a plasmid expressing a GFP-Rab11 fusion-protein, followed by addition of 24p3-Alexa568 and visualization by immunofluorescence microscopy. The results of Figure 4D (upper panel) indicate that much of 24p3-Alexa568 colocalized with GFP-Rab11, indicating that a portion of intracellular 24p3 is associated with recycling endosomes.

To confirm these results, we also analyzed 24p3-Alexa568 localization, following introduction of two proteins that, when overexpressed, alter the intracellular distribution and inhibit the function of recycling endosomes: Rab11-S29F, a dominant-negative Rab11 mutant (Pasqualato et al., 2004), and Rififylin, a component of recycling endosomes (Coumailleau et al., 2004). Figure 4D (middle panel) shows that relative to wild-type GFP-Rab11, GFP-Rab11-S29F assumed a more condensed, perinuclear distribution, consistent with previous results (Pasqualato et al., 2004). Significantly, GFP-Rab11-S29F altered the distribution of and colocalized with 24p3-Alexa568. As expected from previous studies (Coumailleau et al., 2004), expression of GFP-Rififylin also resulted in perinuclear accumulation of the recycling endosome compartment (Figure 4D, lower panel). Likewise, GFP-Rififylin altered the distribution of and colocalized with 24p3-Alexa568.

We next sought to verify that 24p3-mediated iron export required recycling endosome function. HeLa/X7 and HeLa/24p3R-L cells were transfected with a plasmid expressing GFP-Rab11-S29F or GFP-Rififylin. The cells were then preincubated with ^{55}Fe, and the ability of DFO or apo-24p3 to transfer intracellular iron to the extracellular medium was analyzed. The results of Figure 4E show that addition of DFO to either HeLa/X7 or HeLa/24p3R-L cells resulted in the accumulation of ^{55}Fe in the extracellular medium, which was unaffected by Rab11-S29F or Rififylin. By contrast, apo-24p3 promoted the accumulation of ^{55}Fe in the extracellular medium only in HeLa/24p3R-L cells; this accumulation was inhibited by both Rab11-S29F and Rififylin. Thus, recycling endosome function is required for 24p3-mediated iron export.

As mentioned above, 24p3 binds iron through an associated siderophore (Yang et al., 2002). We therefore sought to identify the step in the 24p3-mediated intracellular iron-depletion pathway where 24p3 becomes siderophore associated. We first asked whether the 24p3 present in CM from IL-3-deprived FL5.12 cells was able to bind iron. ^{55}Fe was

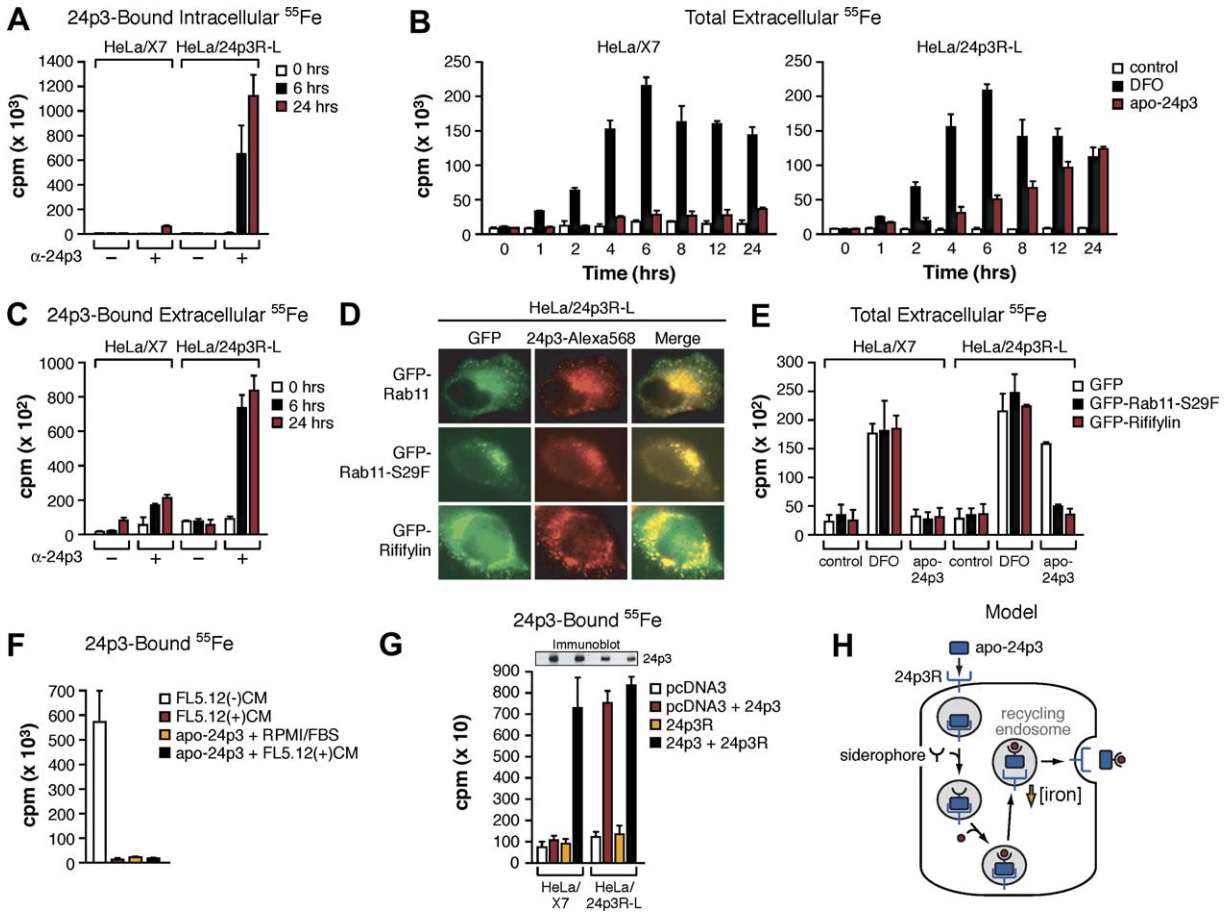

Figure 4. The 24p3-Mediated Intracellular Iron Depletion Pathway

(A) Analysis of 24p3 association with intracellular ^{55}Fe. Cells were preincubated with ^{55}Fe, recultured in fresh medium lacking ^{55}Fe, and then treated with apo-24p3. Cell lysates were immunoprecipitated with an anti-24p3 antibody (α-24p3) or, as a negative control, rabbit serum 0, 6, or 24 hr following apo-24p3 treatment. Error bars represent standard deviation.

(B) Analysis of ^{55}Fe transfer to the extracellular medium. Cells were treated as described in (A), and the accumulation of ^{55}Fe in the medium was analyzed after addition of apo-24p3 or DFO.

(C) Analysis of 24p3 association with extracellular ^{55}Fe. Cells were treated as described in (A), washed to remove extracellular apo-24p3, and the extracellular medium was immunoprecipitated with α-24p3 or rabbit serum 0, 6, or 24 hr later.

(D) Localization of intracellular 24p3 to recycling endosomes. HeLa/24p3R-L cells were electroporated with GFP-Rab11, GFP-Rab11-S29F, or GFP-Rifilylin expression plasmids. After 6 hr, cells were incubated with 24p3-Alexa568 for 40 min in medium containing 1% serum, and after washing and fixation they were examined by fluorescence microscopy.

(E) Dependence of 24p3-mediated iron export on recycling endosome function. HeLa/X7 and HeLa/24p3R-L cells were transfected with a GFP, GFP-Rab11-S29F, or GFP-Rifilylin expression plasmid, loaded with ^{55}Fe, and following a 2 hr incubation with 24p3 or DFO, transfer of iron to the extracellular medium was measured.

(F) 24p3 associates with the siderophore intracellularly. ^{55}Fe was added to FL5.12(-)CM and FL5.12(+)CM or to various control media in combination with apo-24p3, and association with 24p3 in the media was determined by immunoprecipitation.

(G) Association of 24p3 with the siderophore is dependent upon 24p3R. (Top) Immunoblot analysis for 24p3 in the CM. (Bottom) ^{55}Fe was added to HeLa/X7 and HeLa/24p3R-L cells transfected with a control, 24p3 and/or 24p3R expression plasmid, and association with 24p3 in the CM was determined by immunoprecipitation.

(H) Schematic summary of the 24p3-mediated intracellular iron depletion pathway.

added to CM from FL5.12 cells cultured in the absence or presence of IL-3 [FL5.12(-)CM or FL5.12(+)CM, respectively] or various control media, and association with 24p3 was determined by immunoprecipitation. The results of Figure 4F indicate that the 24p3 in FL5.12(-)CM was siderophore associated, as evidenced by its ability to bind ^{55}Fe. However, when recombinant apo-24p3 was added to fresh, unconditioned medium or to FL5.12(+)CM, binding of ^{55}Fe was not detected, indicating that the siderophore is not present in the extracellular medium. Collectively, these results indicate that apo-24p3 associates with the siderophore intracellularly.

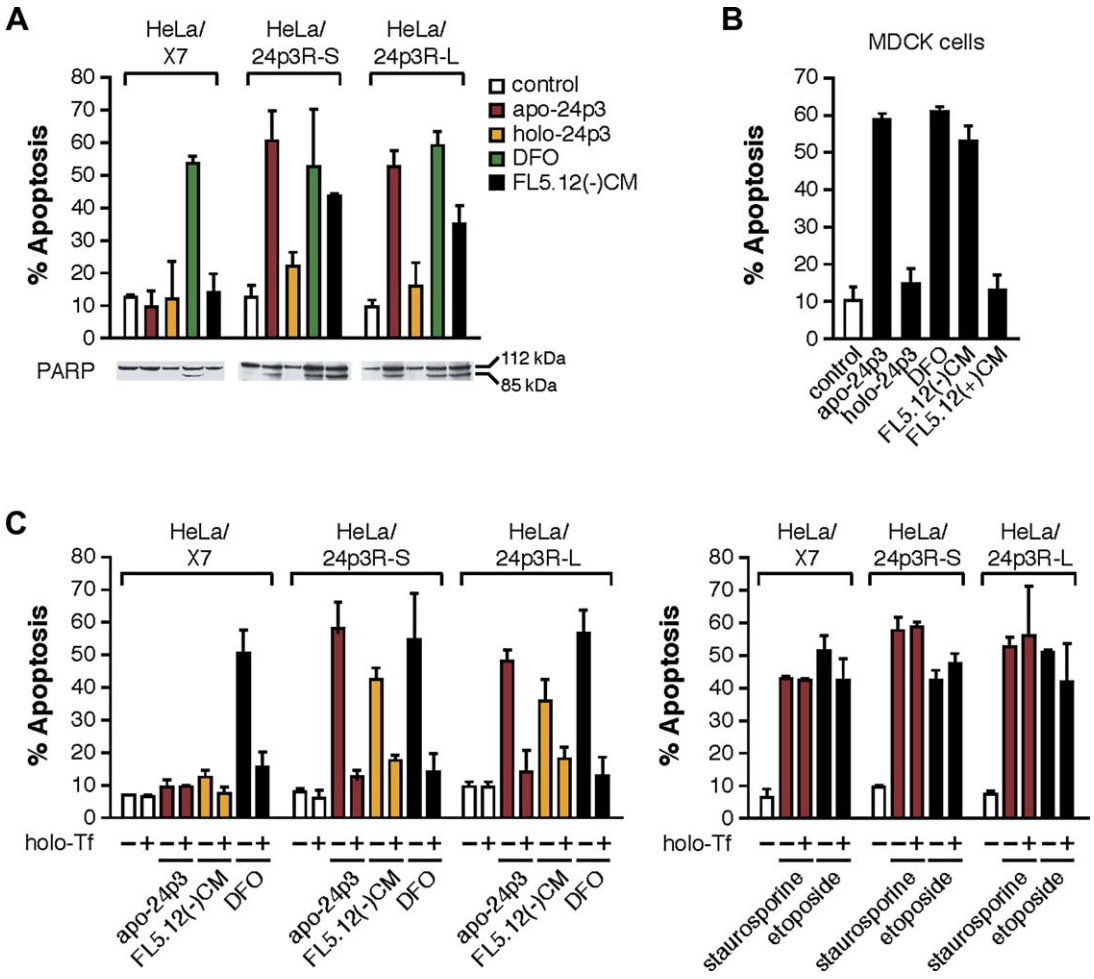

Figure 5. 24p3-Mediated Apoptosis in Cells Expressing 24p3R

(A) Apoptosis was quantitated by annexin V-FITC staining (top) or immunoblot analysis of PARP cleavage (bottom). Apoptosis and PARP cleavage were analyzed 72 and 24 hr after treatment, respectively. Error bars represent standard deviation.

(B) Apoptosis was monitored in MDCK cells by annexin V-FITC staining 48 hr after treatment.

(C) Holo-Tf was analyzed for its ability to block apoptosis 48 hr after addition of apo-24p3, FL5.12(-)CM, or DFO (left) or 24 hr after addition of staurosporine or etoposide (right).

The finding that 24p3 associates with the siderophore intracellularly raised the possibility that this event was promoted by internalization of 24p3 through 24p3R. To test this idea, HeLa/X7 and HeLa/24p3R-L cells were transiently transfected with a plasmid expressing 24p3, and after 48 hr the 24p3 in the CM was tested for its ability to bind ^{55}Fe. Figure 4G shows that CM from HeLa/X7 and HeLa/24p3R-L cells contained comparable amounts of 24p3 (top). However, only the 24p3 in CM from HeLa/24p3R-L cells was able to bind ^{55}Fe (bottom), indicating that the 24p3 in CM from HeLa/24p3R-L cells but not HeLa/X7 cells was siderophore associated. Coexpression of 24p3R in HeLa/X7 cells substantially increased the ability of 24p3 to bind ^{55}Fe. These results suggest that following synthesis, apo-24p3 is initially secreted in a siderophore-free state and associates with the siderophore intracellularly following endocytosis. Based upon the results of Figure 4 and the general paradigm of other endocytosed ligand-receptor complexes (Maxfield and McGraw, 2004), we propose a pathway for 24p3-mediated iron depletion that is summarized in Figure 4H.

24p3-Mediated Apoptosis in Cells Expressing 24p3R

We next examined the ability of 24p3R to mediate 24p3-dependent apoptosis. The different preparations of 24p3 were added to the three HeLa cell lines, and apoptosis was analyzed by annexin V-FITC staining. Figure 5A shows that apo-24p3 and FL5.12(-)CM induced apoptosis in HeLa/24p3R-S and HeLa/24p3R-L cells but not in HeLa/X7 cells. We confirmed that cell death was due to apoptosis by analyzing proteolytic cleavage of poly(ADP-ribose) polymerase (PARP) (Figure 5A, bottom). By contrast, addition of holo-24p3 failed to induce apoptosis in HeLa/24p3R-S and HeLa/24p3R-L cells. As expected from previous studies (reviewed

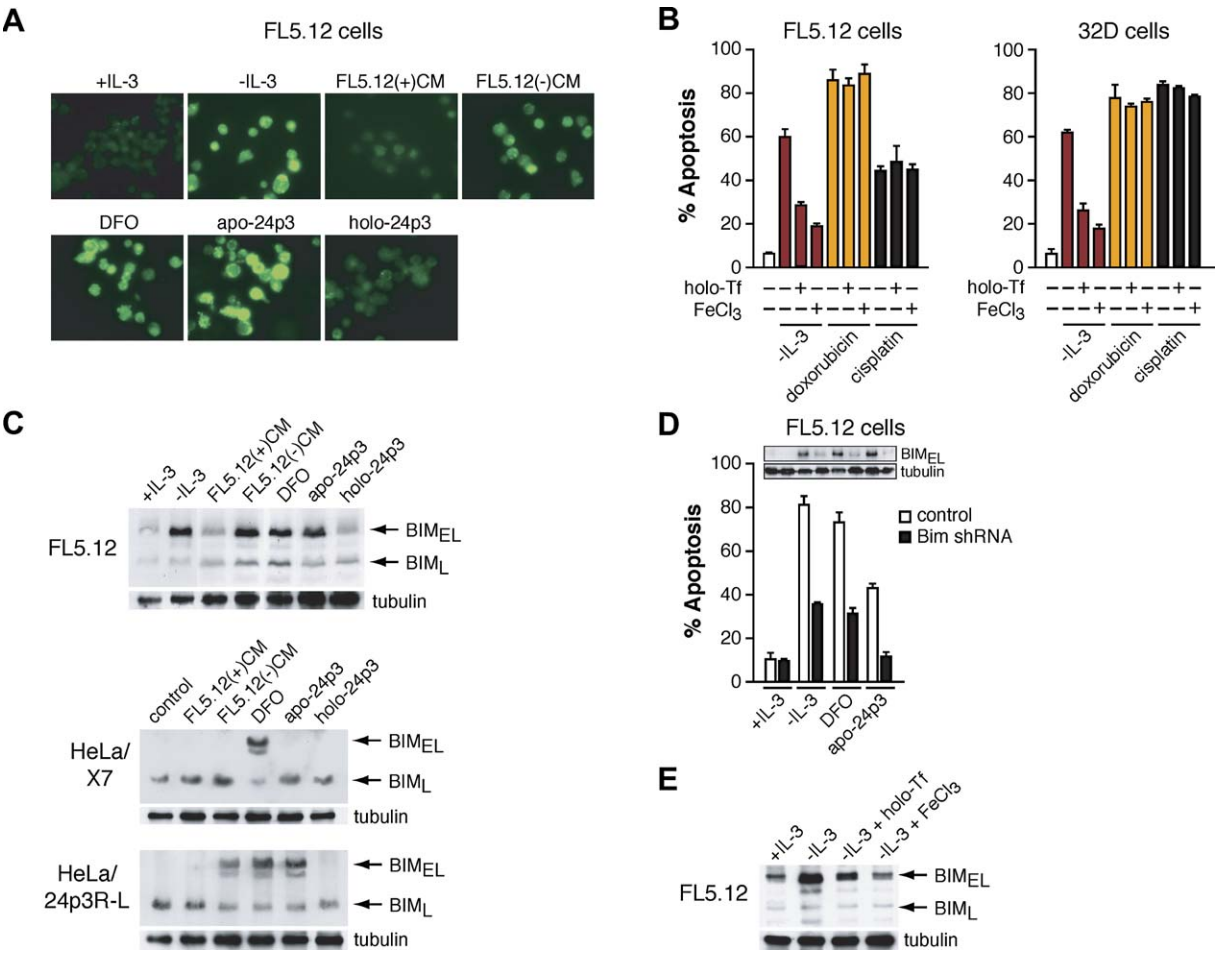

Figure 6. Apoptosis due to IL-3 Deprivation is Regulated by Intracellular Iron Levels and Involves Induction of Bim

(A) Determination of intracellular iron concentration by fluorescence calcein assay.

(B) Apoptosis assays. Holo-Tf and $FeCl_3$ were analyzed for their ability to block apoptosis 1 hr after IL-3 deprivation or after addition of doxorubicin or cisplatin. Error bars represent standard deviation.

(C) Immunoblot analysis of Bim levels.

(D) Suppression of apoptosis by a Bim shRNA.

(E) Immunoblot analysis of Bim levels.

in Le and Richardson, 2002), the iron chelator DFO induced apoptosis in all three cell lines. Identical results were obtained in MDCK kidney cells (Figure 5B), which contain high levels of 24p3R (see Figure 1D) and have been previously used to study 24p3-mediated iron delivery (Yang et al., 2002).

The above results indicate that apo-24p3 and FL5.12(-)CM decrease intracellular iron levels and induce apoptosis in cells expressing 24p3R. It is well established that iron chelators can induce apoptosis (Le and Richardson, 2002). We reasoned that if the basis of 24p3-mediated apoptosis was in fact decreased intracellular iron concentration, then cell death should be prevented by delivery of iron through an alternative pathway. To test this prediction, we analyzed the ability of holo-Tf to block 24p3-mediated apoptosis. The results indicate that holo-Tf suppressed apoptosis induced by either apo-24p3, FL5.12(-)CM, or DFO (Figure 5C, left). By contrast, holo-Tf had no effect on apoptosis induced by staurosporine, a protein kinase C inhibitor, or etoposide, a DNA-damaging agent (Figure 5C, right).

Regulation of Apoptosis due to IL-3 Deprivation through Intracellular Iron Levels

Following cytokine deprivation, IL-3-dependent cell lines, such as FL5.12 cells, synthesize and secrete 24p3 (Devireddy et al., 2001). The similar behavior of recombinant apo-24p3 and FL5.12(-)CM in the experiments described in Figures 3 and 5 suggested that the majority of 24p3 in the FL5.12(-)CM was in the apo form. We therefore predicted that intracellular iron levels in FL5.12 cells would decrease following IL-3 deprivation. To test this prediction, we measured intracellular iron levels in FL5.12 cells in the presence or absence of IL-3 using the fluorescence calcein assay. The results of Figure 6A show that in calcein-loaded FL5.12 cells there was a large increase in fluorescence

emission following withdrawal of IL-3 or addition of DFO, apo-24p3, or FL5.12(-)CM. Thus, in FL5.12 cells, IL-3 deprivation leads to reduced intracellular iron levels. To confirm that reduced intracellular iron levels contributed to apoptosis, we analyzed the ability of holo-Tf or ferric chloride ($FeCl_3$) to block apoptosis following IL-3 deprivation. The results of Figure 6B show that addition of either holo-Tf or $FeCl_3$ significantly suppressed apoptosis in IL-3-deprived FL5.12 cells. By contrast, holo-Tf or $FeCl_3$ had no effect on FL5.12 cell apoptosis induced by the DNA-damaging agents doxorubicin and cisplatin. Identical results were obtained in 32D cells, another IL-3-dependent cell line.

Induction of the BH3-Only Protein Bim by IL-3 Deprivation, Apo-24p3, and Iron Chelators

We next sought to understand how a reduction in intracellular iron levels functioned through the core apoptotic machinery to promote cell death. Previous studies have shown that cytokine deprivation of IL-3-dependent cell lines results in the induction (Kuribara et al., 2004; Shinjyo et al., 2001) and posttranslational activation (Harada et al., 2004) of Bim, a BH3-only proapoptotic member of the Bcl-2 family (reviewed in Strasser et al., 2000). Ectopic expression of Bim induces apoptosis (Shinjyo et al., 2001) and, conversely, small interfering RNA (siRNA) mediated Bim knockdown suppresses apoptosis following IL-3 deprivation (Harada et al., 2004).

These considerations prompted us to investigate the role of Bim in 24p3- and iron chelator-mediated apoptosis. The immunoblot of Figure 6C shows, consistent with previous studies (Kuribara et al., 2004), that IL-3 deprivation of FL5.12 cells resulted in increased levels of a spliced variant of Bim, called Bim extra-long (BimEL). Significantly, addition of apo-24p3, FL5.12(-)CM, or DFO resulted in a comparable increase of BimEL levels in FL5.12 and HeLa/24p3R-L cells, whereas in HeLa/X7 cells BimEL levels were increased only by DFO.

To confirm that BimEL induction was required for apoptosis, we performed RNA interference (RNAi) experiments. We derived an FL5.12 cell line stably expressing a small hairpin RNA (shRNA) directed against Bim. Figure 6D shows that the Bim shRNA substantially reduced apoptosis following IL-3 deprivation, consistent with previous results (Harada et al., 2004). Significantly, the Bim shRNA also suppressed apoptosis resulting from addition of DFO or apo-24p3. Immunoblot analysis confirmed that the Bim shRNA efficiently and selectively reduced BimEL levels. These results indicate that induction of BimEL is required for efficient apoptosis resulting from IL-3 deprivation or addition of DFO or apo-24p3.

The results of Figures 6A–6C suggested that in IL-3-deprived cells, Bim expression is induced in response to decreased intracellular iron levels. A prediction of this idea is that intracellular iron delivery would suppress the induction of Bim expression that normally occurs following IL-3 deprivation. Figure 6E shows that in IL-3-deprived FL5.12 cells, addition of holo-Tf or $FeCl_3$ substantially decreased Bim induction in a manner that correlated with the decreased apoptosis (Figure 6B).

Reciprocal Misregulation of *24p3* and *24p3R* Expression by BCR-ABL

Certain oncoproteins can render cells growth factor independent, which is related to their ability to prevent apoptosis and promote cell survival. For example, BCR-ABL as well as some other oncogenic tyrosine kinases can confer resistance to apoptosis in cytokine-deprived, IL-3-dependent mouse cell lines (reviewed in Cross and Reiter, 2002; Skorski, 2002). Because *24p3* is normally transcriptionally activated following IL-3 deprivation, BCR-ABL must counteract the expression or function of the 24p3/24p3R proapoptotic pathway.

To investigate this issue, we first analyzed expression of *24p3* in IL-3-dependent murine 32D and BaF3 cells and in 32D and BaF3 cells expressing BCR-ABL (32D/BCR-ABL and BaF3/BCR-ABL, respectively) (Nieborowska-Skorska et al., 1999; Okuda et al., 1996). As expected from our previous study (Devireddy et al., 2001), in parental 32D and BaF3 cells, *24p3* was expressed only following IL-3 deprivation (Figure 7A). Unexpectedly, in 32D/BCR-ABL and BaF3/BCR-ABL cells, *24p3* was constitutively expressed regardless of whether IL-3 was present. To confirm that expression of *24p3* in 32D/BCR-ABL and BaF3/BCR-ABL cells was due to BCR-ABL, we treated cells with the BCR-ABL inhibitor, imatinib mesylate (also called STI-571 or Gleevec). Figure 7B shows that addition of imatinib virtually eliminated *24p3* expression in 32D/BCR-ABL and BaF3/BCR-ABL cells, verifying the involvement of BCR-ABL.

The expression data of Figure 7A predict that CM from 32D/BCR-ABL and BaF3/BCR-ABL cells should contain 24p3 and induce apoptosis in parental 32D and BaF3 cells, which are sensitive to 24p3-mediated apoptosis (Devireddy et al., 2001). Consistent with this prediction, Figure 7C shows that CM from 32D/BCR-ABL and BaF3/BCR-ABL cells induced apoptosis following addition to 32D or BaF3 cells.

The finding that 32D/BCR-ABL and BaF3/BCR-ABL cells expressed and secreted 24p3 but were viable raised the possibility that expression or function of 24p3R might be inhibited. Figure 7D shows, as expected, that *24p3R* was expressed in the parental 32D and BaF3 cells regardless of whether IL-3 was present. Significantly, however, *24p3R* expression was substantially reduced in 32D/BCR-ABL and BaF3/BCR-ABL cells. To confirm that the decreased expression of *24p3R* in 32D/BCR-ABL and BaF3/BCR-ABL cells was due to BCR-ABL, we analyzed the effect of imatinib addition. The results of Figure 7E show that following addition of imatinib to 32D/BCR-ABL and BaF3/BCR-ABL cells cultured in the presence of IL-3, *24p3R* expression increased dramatically to levels approximating those observed in the parental cells. Imatinib also increased expression of *24p3R* and decreased expression of *24p3* in 32D/BCR-ABL and BaF3/BCR-ABL cells cultured in the absence of IL-3 (Figure 7F).

Collectively, the results of the expression analyses suggested that 32D/BCR-ABL and BaF3/BCR-ABL cells were viable because *24p3R* expression was downregulated. A prediction of this idea is that ectopic expression of *24p3R* in 32D/BCR-ABL and BaF3/BCR-ABL cells would induce cell death. Figure 7G shows that transfection of a *24p3R*-expression plasmid induced apoptosis in 32D/BCR-ABL and

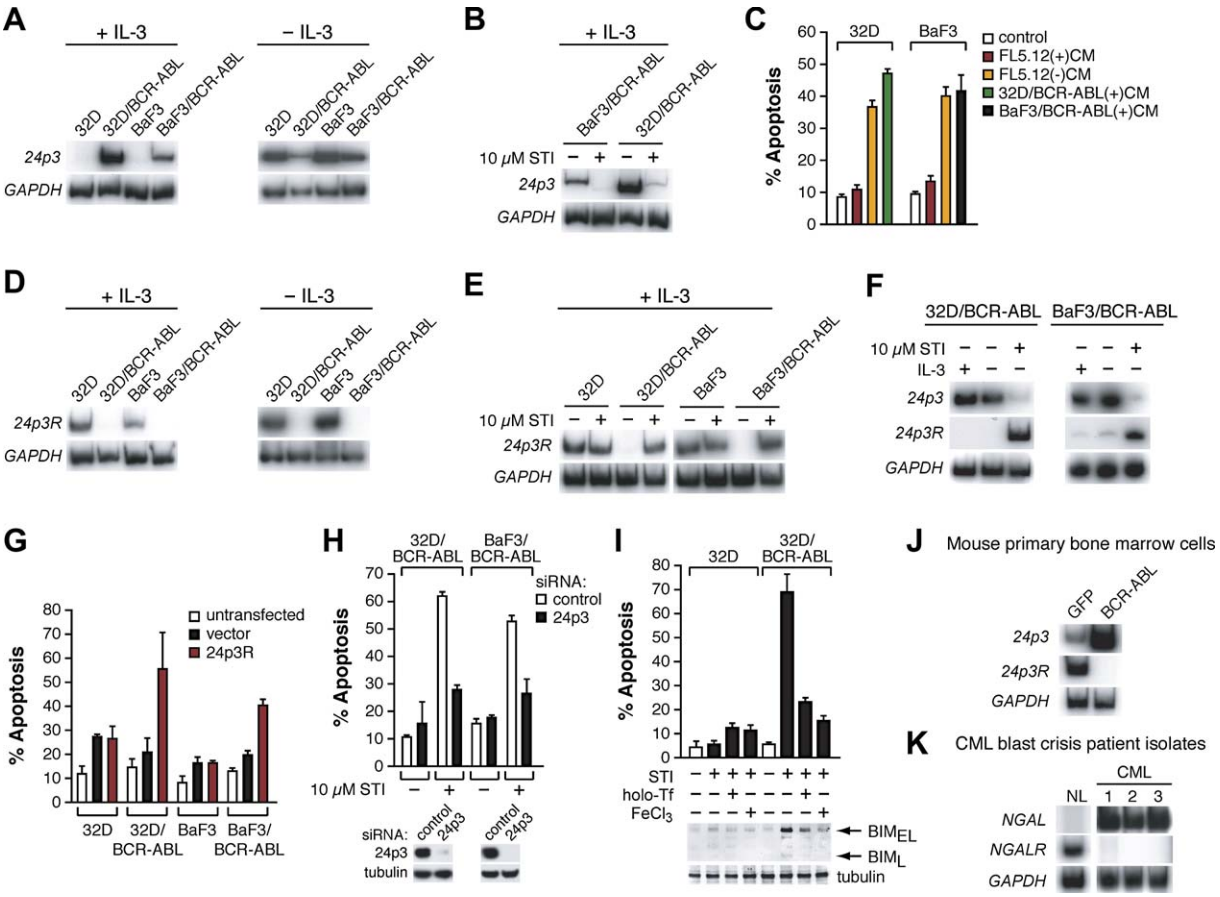

Figure 7. Reciprocal Misregulation of *24p3* and *24p3R* Expression by BCR-ABL

(A) RT-PCR analysis of *24p3* expression in parental 32D or BaF3 cells and in 32D and BaF3 cells expressing BCR-ABL (32D/BCR-ABL and BaF3/BCR-ABL, respectively) in the presence or absence of IL-3.

(B) RT-PCR analysis of *24p3* expression in 32D/BCR-ABL and BaF3/BCR-ABL cells 8 hr following treatment with 10 μM imatinib (STI).

(C) Apoptosis assays. Apoptosis was analyzed in 32D and BaF3 cells cultured in FL5.12(-)CM, FL5.12(+)CM, 32D/BCR-ABL(+)CM, or BaF3/BCR-ABL(+)CM for 72 hr. Error bars represent standard deviation.

(D) RT-PCR analysis of *24p3R* expression.

(E and F) RT-PCR analysis following imatinib treatment of 32D/BCR-ABL and BaF3/BCR-ABL cells in the presence or absence of IL-3.

(G) Apoptosis assays. Cells cultured in the presence of IL-3 were transfected with a plasmid expressing *24p3R*, and apoptosis was analyzed 48 hr later.

(H) Suppression of imatinib-mediated apoptosis by a 24p3 siRNA. The 24p3 siRNA was directed against the sequence 5′-AAGGCAGCTTTACGATGTA-3′; the control siRNA (5′-CTTACGCTGAGTACTTCGA-3′) was directed against luciferase.

(I) Apoptosis assays (top) and analysis of Bim levels (bottom) in cells treated with imatinib, holo-Tf, and/or $FeCl_3$.

(J) RT-PCR analysis of *24p3* and *24p3R* expression in primary bone marrow cells transduced with a retrovirus expressing either BCR-ABL or, as a control, GFP.

(K) RT-PCR analysis of *24p3* and *24p3R* expression in peripheral blood mononuclear cells from CML blast crisis patients (CML) or pooled peripheral blood mononuclear cells from normal (NL) volunteers.

BaF3/BCR-ABL cells but not in the parental 32D or BaF3 cells.

Imatinib induces apoptosis in BCR-ABL$^+$ cells (Deininger et al., 2005). Our finding that in BCR-ABL$^+$ cells imatinib increases *24p3R* expression, thus restoring a functional 24p3/24p3R pathway, suggested that this may be the basis of imatinib-mediated apoptosis. To test this idea we first performed an RNAi experiment to determine whether imatinib-mediated apoptosis was dependent upon 24p3. Figure 7H shows that an siRNA directed against 24p3 efficiently reduced 24p3 levels in 32D/BCR-ABL and BaF3/BCR-ABL cells (bottom) and suppressed killing by imatinib (top). We also tested whether intracellular iron delivery would prevent killing of BCR-ABL$^+$ cells by imatinib. Figure 7I shows, as expected, that imatinib efficiently induced apoptosis in 32D/BCR-ABL cells, whereas the parental 32D cells were unaffected. Remarkably, holo-Tf or $FeCl_3$ substantially decreased apoptosis in imatinib-treated 32D/BCR-ABL cells. Consistent with previous results (Kuribara et al., 2004), imatinib treatment of 32D/BCR-ABL cells induced Bim expression

(Figure 7I, bottom). Significantly, addition of holo-Tf or $FeCl_3$ suppressed induction of Bim expression in a manner that correlated with the decreased apoptosis.

We next asked whether BCR-ABL would also misregulate *24p3* and *24p3R* expression in primary cells. Primary mouse bone marrow cells were transduced with a retrovirus expressing BCR-ABL or, as a control, green fluorescent protein (GFP). The results of Figure 7J show that in BCR-ABL-expressing primary bone marrow cells, *24p3* expression was increased and *24p3R* expression was reduced, analogous to the results obtained in the BCR-ABL$^+$ transformed cell lines.

Finally, we performed comparable expression analysis in leukemic blasts isolated from chronic myelogenous leukemia (CML) blast crisis patients. The human homolog of 24p3 is neutrophil gelatinase-associated lipocalin (Ngal) (Bundgaard et al., 1994), and we will refer to the human homolog of 24p3R as NgalR. Figure 7K shows that three independent CML blast isolates expressed high levels of *NGAL* and virtually undetectable levels of *NGALR*, analogous to the results obtained in BCR-ABL$^+$ mouse cells. By contrast, pooled peripheral blood lymphocytes from normal donors expressed high levels of *NGALR* and very low levels of *NGAL*.

DISCUSSION

On the basis of the results in this report and recent studies (Goetz et al., 2002; Yang et al., 2002, 2003), we propose the following model for the distinct activities elicited by 24p3. We have found that the iron status of 24p3 is the critical determinant of its activity. Holo-24p3 binds to 24p3R, is internalized, and releases its bound iron, thereby increasing intracellular iron concentration. By contrast, apo-24p3 binds to 24p3R, is internalized, and following association with an intracellular siderophore, chelates iron and transfers it to the extracellular medium, thereby reducing intracellular iron concentration and resulting in apoptosis (Figure 4H).

24p3-Mediated Apoptosis and Implications for BCR-ABL-Mediated Myeloproliferative Disease

Decreasing intracellular iron levels is known to induce apoptosis and, in fact, iron chelators are currently under investigation as anticancer agents (Le and Richardson, 2002). To our knowledge, however, 24p3/24p3R is the first example of a biological pathway in which apoptosis is regulated through intracellular iron concentration. Our results reveal an unanticipated role for regulation of intracellular iron levels in apoptosis induced by IL-3 deprivation.

We have found that an important aspect of this apoptotic mechanism is induction of the proapoptotic Bim protein in response to decreased intracellular iron. Ectopic expression of Bim can induce apoptosis (Shinjyo et al., 2001), and Bim is required for apoptosis resulting from IL-3 deprivation (Harada et al., 2004; Figure 6D) or addition of apo-24p3 or DFO (Figure 6D). We have found that agents that reduce intracellular iron levels increase BimEL levels. Most importantly, intracellular iron delivery blocks induction of Bim expression and apoptosis following IL-3 deprivation, addition of 24p3, or addition of DFO.

Unexpectedly, we found that in mouse cell lines, BCR-ABL profoundly misregulates expression of both *24p3* and *24p3R*. *24p3* was dramatically upregulated in BCR-ABL$^+$ mouse cell lines, primary mouse cells, and leukemic blasts isolated from CML patients. Consistent with our results, a recent study reported that *24p3* is upregulated in BCR-ABL-transformed mouse cell lines (Lin et al., 2005), and expression profiling identified *NGAL* as one of the genes upregulated in CML leukemic cells (Kaneta et al., 2003). Significantly, we also found that *24p3R* expression is repressed by BCR-ABL. Forced expression of *24p3R* induces apoptosis in BCR-ABL-transformed mouse cell lines, indicating that downregulation of *24p3R* is critical for survival in the presence of the 24p3 secreted in the CM.

Several lines of evidence confirmed that BCR-ABL is responsible for misregulation of *24p3* and *24p3R* expression. First, misregulation was reversed by addition of imatinib, a specific BCR-ABL kinase inhibitor. Second, ectopic expression of BCR-ABL in primary cells resulted in misregulation of *24p3* and *24p3R*. Remarkably, killing of BCR-ABL$^+$ cells by imatinib was blocked by iron delivery, verifying the essential role of the 24p3/24p3R proapoptotic pathway. Consistent with our conclusion, BimEL, which we found is involved in 24p3-mediated apoptosis, has been shown to play a critical role in imatinib-induced cell death (Essafi et al., 2005).

The misregulation of *24p3* and *24p3R* expression by BCR-ABL may be relevant to the severity or progression of CML. Mice injected with BCR-ABL$^+$ cells show atrophy of the bone marrow, characterized by a severe reduction in normal hematopoiesis and eventual death (Lin et al., 2001). Based upon this finding, it has been proposed that BCR-ABL$^+$ cells secrete one or more factors that interfere with normal hematopoiesis and contribute to disease severity (Eaves et al., 1998). 24p3 has the properties expected of this secreted factor, and the downregulation of *24p3R* expression may explain the resistance of BCR-ABL$^+$ cancer cells to apoptosis.

EXPERIMENTAL PROCEDURES

Cell Lines

Stable cell lines expressing N-terminal epitope-tagged derivatives of 24p3R-S or 24p3R-L, or the empty expression vector (X7), were derived by transfection of HeLa cells using FuGene (Roche) and selection with Blasticidin. FL5.12 cells stably expressing a Bim shRNA directed against the sequence 5′-GCCCAGACATTTGGTCAGTTAT-3′ from PSM2 (Open Biosystems) or, as a control, PSM2 were derived by electroporation and puromycin selection. Peripheral blood mononuclear cells from CML blast crisis patients and normal donors were obtained from the human tissue repository at the University of Massachusetts Medical School, and total RNA was prepared using TRIzol reagent (Invitrogen).

Expression Cloning of 24p3R

A cDNA library was synthesized from FL5.12 poly(A)$^+$ mRNA using an oligo-dT primer, and size-selected cDNAs (>1 kb) were directionally cloned into pCMV-SPORT6 (Gibco-BRL). The library was transfected into COS-7 cells, and after 36 hr cells were dislodged in PBS containing 0.5 mM EDTA and resuspended in binding buffer (2% BSA in PBS). The cells were panned on GST-24p3 coated plates (1×10^7 cells/plate) that

were prepared as follows. Bacteriological petri plates (Falcon) were layered with 10 mg/ml anti-mouse IgG (Kirkegaard and Perry Laboratories, Inc.; KPL) in 50 mM Tris-HCl, pH 9.5, rinsed with 0.15 M NaCl, and blocked with BSA blocking buffer (KPL). Anti-GST monoclonal antibody (1 mg/ml) (Santa Cruz Biotechnology) in PBS/2% BSA was added to each dish and incubated overnight at 4ºC. The plates were washed with PBS and incubated with 20 mg of purified GST-24p3. Nonadherent cells were removed by washing with PBS/2% BSA, the adherent cells were lysed with HIRT buffer, and the plasmid DNA was recovered. After three rounds of panning, individual plasmids were purified and transfected into COS-7 cells, which were then screened for their ability to bind ^{32}P-24p3 as described (Devireddy et al., 2001). Inserts from plasmids that conferred binding to ^{32}P-24p3 were sequenced.

Full-length open reading frames (ORFs) for 24p3R-L and 24p3R-S were obtained by PCR amplification using IMAGE Clones 5365976 and 4511663, respectively. The ORFs were cloned into a derivative of pEF6V5-HisB (Invitrogen) containing an N-terminal multi-epitope (FLAG, S-peptide, and Epitope C) tag (X7).

Antibodies and Immunoblotting

A polyclonal rabbit α-24p3R antibody was raised using a C-terminal 24p3R peptide (CDHVPLLATPNAL) as the immunogen and affinity-purified on a peptide-coupled Sepharose column. Other antibodies were obtained as follows: 24p3 (Santa Cruz Biotechnology), ferritin (Sigma), PARP (BIOMOL), HIF-1α (Santa Cruz Biotechnology), α-tubulin (Sigma), and Bim (Calbiochem).

24p3 Binding and Internalization Assays

HeLa cells (~5×10^5) constitutively expressing 24p3R were treated with 5×10^6 cpm ^{32}P-24p3 and analyzed for binding (Devireddy et al., 2001). For internalization assays, ~5×10^5 cells were treated with 1×10^6 cpm ^{32}P-24p3 and at various time points washed three times with PBS and incubated for 15 min in a solution of Proteinase K, trypsin, and EDTA to remove the extracellular portion of the receptor. Dislodged cells were then collected, washed, and counted using a Beckman Liquid Scintillation counter.

Purification and Labeling of Recombinant 24p3

Full-length 24p3 cDNA was cloned into pGEX2TK (Pharmacia) and expressed in *E. coli* strains XL1 Blue (Stratagene) or BL21 (Pharmacia). XL1 Blue constitutively expresses the siderophore enterobactin, and thus 24p3 derived from this strain is iron loaded (holo-24p3); BL21 lacks enterobactin, and 24p3 derived from this strain lacks iron (apo-24p3) (Goetz et al., 2002). Following induction with 1 mM IPTG (Promega), bacteria were lysed, and recombinant 24p3 was purified as described (Bundgaard et al., 1994).

To prepare ^{32}P-labeled 24p3, GST-24p3-Sepharose beads were incubated with ^{32}P-γATP (New England Nuclear) in 1 × HMK buffer (20 mM Tris-HCl pH 7.5, 100 mM NaCl, 12 mM MgCl2) containing 5 U of bovine heart muscle kinase (Sigma) for 30 min at 4ºC, washed five times with 10 volumes of 1 × PBS, and incubated with thrombin to cleave the labeled 24p3. To generate Alexa568-derivatized 24p3, GST-24p3 was immobilized on glutathione agarose (250 μl) in a solution of 500 μl PBS, 0.1M $NaHCO_3$, and 250 μg Alexa568 (Molecular Probes) for 30 min at room temperature. After extensive washing to remove the unreacted dye, labeled 24p3 was cleaved from the beads using 3 U thrombin (Sigma) in 250 μl PBS for 6 hr at room temperature, and the reaction was stopped by adding 0.1 mM AEBSF.

Immunofluorescence

For confocal microscopy, 24p3-Alexa568 (10 μg/ml) was added to ~2.5×10^5 chilled cells and incubated for 1 hr at 4ºC followed by 1 hr at 37ºC. Cells were washed ten times with PBS, fixed in 4% paraformaldehyde in PBS, washed in water, and mounted on a glass slide. For Rab11/Rififylin colocalization experiments, 1×10^6 cells were transfected with 2 μg of a plasmid expressing a GFP fusion protein using the Amaxa electroporator and plated on rat tail collagen-treated coverslips in DMEM+ 10% FCS. Six hours later, cells were incubated in DMEM + 1% FCS and 100 μg/ml of 24p3-Alexa568 for 45 min. Coverslips were washed three times with complete medium, three times with cold PBS, fixed with 4% paraformaldehyde in PBS for 30 min, treated with 0.1% sodium borohydride for 20 min, rinsed extensively in PBS, mounted in 90% glycerol, 2% DABCO, 10 mM Tris pH 7.5, and examined with a Zeiss Axioplan2 microscope.

Intracellular and Extracellular Iron Determination

Colorimetric determination of intracellular iron was measured using ferrozine (Sigma) as described (Leardi et al., 1998). For calcein assays, cells were stained with 0.5 μM Calcein-AM (Molecular Probes) in RPMI (without phenol red and FBS) for 10 min at room temperature and then washed three times with RPMI (without phenol red and FBS). Washed cells were deposited onto glass slides by cytospin, mounted using a mounting medium (Vector Labs), and observed under a fluorescent microscope. In most experiments, cells were incubated with 50 μg/ml holo- or apo-24p3, 50 μM $FeCl_3$, 100 μg/ml holo-Tf, or 100 μM DFO (Calbiochem).

For analysis of 24p3 bound intracellular iron, cells were washed once with ice-cold PBS and lysed with 0.1% Triton-X 100 in PBS for 15 min on ice. Clarified cell lysate was incubated with 0.2 μg of 24p3 antibody overnight at 4ºC, followed by incubation with washed Protein A agarose beads (Santa Cruz Biotechnology) for 4 hr at 4ºC. Beads were collected by centrifugation and washed three times with PBS and three times with PBS containing 0.1% Triton-X 100 and then subjected to liquid scintillation counting. For analysis of 24p3 bound extracellular iron, extracellular medium was immunoprecipitated and analyzed as described above. For analysis of total extracellular iron, the counts per minute (cpm) of the extracellular medium were determined by liquid scintillation counting.

ACKNOWLEDGMENTS

We thank D. Goetz for advice on 24p3 purification; M. Cohen-Tannoudji for the Rififylin construct; R. Bruick for the *NIP3*-Luciferase reporter plasmid; T. Skorski for 32D/BCR-ABL cells; K. Okuda for BaF3/BCR-ABL cells; A. Raza, N. Galili, and M. Stevenson for peripheral blood samples; and S. Evans for editorial assistance. This work was supported by grants from the Leukemia and Lymphoma Society (L.R.D.) and the Centre National de la Recherche Scientifique (C.G.). M.R.G. is an investigator of the Howard Hughes Medical Institute.

Received: April 26, 2005
Revised: August 23, 2005
Accepted: October 11, 2005
Published: December 28, 2005

REFERENCES

Akerstrom, B., Flower, D.R., and Salier, J.P. (2000). Lipocalins: unity in diversity. Biochim. Biophys. Acta *1482*, 1–8.

Bundgaard, J.R., Sengelov, H., Borregaard, N., and Kjeldsen, L. (1994). Molecular cloning and expression of a cDNA encoding NGAL: a lipocalin expressed in human neutrophils. Biochem. Biophys. Res. Commun. *202*, 1468–1475.

Chong, T.W., Horwitz, L.D., Moore, J.W., Sowter, H.M., and Harris, A.L. (2002). A mycobacterial iron chelator, desferri-exochelin, induces hypoxia-inducible factors 1 and *2*, NIP3, and vascular endothelial growth factor in cancer cell lines. Cancer Res. *62*, 6924–6927.

Cohen, J.J., and Duke, R.C. (1984). Glucocorticoid activation of a calcium-dependent endonuclease in thymocyte nuclei leads to cell death. J. Immunol. *132*, 38–42.

Coumailleau, F., Das, V., Alcover, A., Raposo, G., Vandormael-Pournin, S., Le Bras, S., Baldacci, P., Dautry-Varsat, A., Babinet, C., and Cohen-Tannoudji, M. (2004). Over-expression of Rififylin, a new RING finger and FYVE-like domain-containing protein, inhibits recycling from the endocytic recycling compartment. Mol. Biol. Cell *15*, 4444–4456.

Cross, N.C., and Reiter, A. (2002). Tyrosine kinase fusion genes in chronic myeloproliferative diseases. Leukemia *16*, 1207–1212.

Datta, S.R., Brunet, A., and Greenberg, M.E. (1999). Cellular survival: a play in three Akts. Genes Dev. *13*, 2905–2927.

Deininger, M., Buchdunger, E., and Druker, B.J. (2005). The development of imatinib as a therapeutic agent for chronic myeloid leukemia. Blood *105*, 2640–2653.

Devireddy, L.R., Teodoro, J.G., Richard, F.A., and Green, M.R. (2001). Induction of apoptosis by a secreted lipocalin that is transcriptionally regulated by IL-3 deprivation. Science *293*, 829–834.

Eaves, C., Cashman, J., and Eaves, A. (1998). Defective regulation of leukemic hematopoiesis in chronic myeloid leukemia. Leuk. Res. *22*, 1085–1096.

Epsztejn, S., Kakhlon, O., Glickstein, H., Breuer, W., and Cabantchik, I. (1997). Fluorescence analysis of the labile iron pool of mammalian cells. Anal. Biochem. *248*, 31–40.

Essafi, A., de Mattos, S.F., Hassen, Y.A., Soeiro, I., Mufti, G.J., Thomas, N.S., Medema, R.H., and Lam, E.W. (2005). Direct transcriptional regulation of Bim by FoxO3a mediates STI571-induced apoptosis in Bcr-Abl-expressing cells. Oncogene *24*, 2317–2329.

Flower, D.R. (1996). The lipocalin protein family: structure and function. Biochem. J. *318*, 1–14.

Galili, U., Leizerowitz, R., Moreb, J., Gamliel, H., Gurfel, D., and Polliack, A. (1982). Metabolic and ultrastructural aspects of the in vitro lysis of chronic lymphocytic leukemia cells by glucocorticoids. Cancer Res. *42*, 1433–1440.

Goetz, D.H., Holmes, M.A., Borregaard, N., Bluhm, M.E., Raymond, K.N., and Strong, R.K. (2002). The neutrophil lipocalin NGAL is a bacteriostatic agent that interferes with siderophore-mediated iron acquisition. Mol. Cell *10*, 1033–1043.

Harada, H., Quearry, B., Ruiz-Vela, A., and Korsmeyer, S.J. (2004). Survival factor-induced extracellular signal-regulated kinase phosphorylates BIM, inhibiting its association with BAX and proapoptotic activity. Proc. Natl. Acad. Sci. USA *101*, 15313–15317.

Ishida, Y., Agata, Y., Shibahara, K., and Honjo, T. (1992). Induced expression of PD-1, a novel member of the immunoglobulin gene superfamily, upon programmed cell death. EMBO J. *11*, 3887–3895.

Kaneta, Y., Kagami, Y., Tsunoda, T., Ohno, R., Nakamura, Y., and Katagiri, T. (2003). Genome-wide analysis of gene-expression profiles in chronic myeloid leukemia cells using a cDNA microarray. Int. J. Oncol. *23*, 681–691.

Kuribara, R., Honda, H., Matsui, H., Shinjyo, T., Inukai, T., Sugita, K., Nakazawa, S., Hirai, H., Ozawa, K., and Inaba, T. (2004). Roles of Bim in apoptosis of normal and Bcr-Abl-expressing hematopoietic progenitors. Mol. Cell. Biol. *24*, 6172–6183.

Le, N.T., and Richardson, D.R. (2002). The role of iron in cell cycle progression and the proliferation of neoplastic cells. Biochim. Biophys. Acta *1603*, 31–46.

Leardi, A., Caraglia, M., Selleri, C., Pepe, S., Pizzi, C., Notaro, R., Fabbrocini, A., De Lorenzo, S., Musico, M., Abbruzzese, A., et al. (1998). Desferioxamine increases iron depletion and apoptosis induced by ara-C of human myeloid leukaemic cells. Br. J. Haematol. *102*, 746–752.

Lenardo, M., Chan, K.M., Hornung, F., McFarland, H., Siegel, R., Wang, J., and Zheng, L. (1999). Mature T lymphocyte apoptosis–immune regulation in a dynamic and unpredictable antigenic environment. Annu. Rev. Immunol. *17*, 221–253.

Lin, F., Monaco, G., Sun, T., Liu, J., Lin, H., Stephens, C., Belmont, J., and Arlinghaus, R.B. (2001). BCR gene expression blocks Bcr-Abl induced pathogenicity in a mouse model. Oncogene *20*, 1873–1881.

Lin, H., Monaco, G., Sun, T., Ling, X., Stephens, C., Xie, S., Belmont, J., and Arlinghaus, R. (2005). Bcr-Abl-mediated suppression of normal hematopoiesis in leukemia. Oncogene *24*, 3246–3256.

Maxfield, F.R., and McGraw, T.E. (2004). Endocytic recycling. Nat. Rev. Mol. Cell Biol. *5*, 121–132.

Nieborowska-Skorska, M., Wasik, M.A., Slupianek, A., Salomoni, P., Kitamura, T., Calabretta, B., and Skorski, T. (1999). Signal transducer and activator of transcription (STAT)5 activation by BCR/ABL is dependent on intact Src homology (SH)3 and SH2 domains of BCR/ABL and is required for leukemogenesis. J. Exp. Med. *189*, 1229–1242.

Okuda, K., Golub, T.R., Gilliland, D.G., and Griffin, J.D. (1996). p210BCR/ABL, p190BCR/ABL, and TEL/ABL activate similar signal transduction pathways in hematopoietic cell lines. Oncogene *13*, 1147–1152.

Pasqualato, S., Senic-Matuglia, F., Renault, L., Goud, B., Salamero, J., and Cherfils, J. (2004). The structural GDP/GTP cycle of Rab11 reveals a novel interface involved in the dynamics of recycling endosomes. J. Biol. Chem. *279*, 11480–11488.

Polyak, K., Xia, Y., Zweier, J.L., Kinzler, K.W., and Vogelstein, B. (1997). A model for p53-induced apoptosis. Nature *389*, 300–305.

Rouault, T., and Klausner, R. (1997). Regulation of iron metabolism in eukaryotes. Curr. Top. Cell. Regul. *35*, 1–19.

Shinjyo, T., Kuribara, R., Inukai, T., Hosoi, H., Kinoshita, T., Miyajima, A., Houghton, P.J., Look, A.T., Ozawa, K., and Inaba, T. (2001). Downregulation of Bim, a proapoptotic relative of Bcl-2, is a pivotal step in cytokine-initiated survival signaling in murine hematopoietic progenitors. Mol. Cell. Biol. *21*, 854–864.

Skorski, T. (2002). Oncogenic tyrosine kinases and the DNA-damage response. Nat. Rev. Cancer *2*, 351–360.

Strasser, A., Puthalakath, H., Bouillet, P., Huang, D.C., O'Connor, L., O'Reilly, L.A., Cullen, L., Cory, S., and Adams, J.M. (2000). The role of bim, a proapoptotic BH3-only member of the Bcl-2 family in cell-death control. Ann. N Y Acad. Sci. *917*, 541–548.

Vaux, D.L., and Korsmeyer, S.J. (1999). Cell death in development. Cell *96*, 245–254.

Wojnar, P., Lechner, M., and Redl, B. (2003). Antisense down-regulation of lipocalin-interacting membrane receptor expression inhibits cellular internalization of lipocalin-1 in human NT2 cells. J. Biol. Chem. *278*, 16209–16215.

Yang, J., Goetz, D., Li, J.Y., Wang, W., Mori, K., Setlik, D., Du, T., Erdjument-Bromage, H., Tempst, P., Strong, R., and Barasch, J. (2002). An iron delivery pathway mediated by a lipocalin. Mol. Cell *10*, 1045–1056.

Yang, J., Mori, K., Li, J.Y., and Barasch, J. (2003). Iron, lipocalin, and kidney epithelia. Am. J. Physiol. Renal Physiol. *285*, F9–F18.